Observations of Diurnal Variation in a Cloud-capped Marine Boundary Layer

P. HIGNETT

Meteorological Office Research Unit, Cardington, Bedfordshire, United Kingdom

(Manuscript received 5 September 1990, in final form 14 January 1991)

ABSTRACT

Observations are presented of the turbulent structure of a cloud-capped boundary layer during the 1987 FIRE marine stratocumulus project. The measurements were made from San Nicolas Island, off the coast of California, using instruments attached to the cable of a tethered balloon. A marked diurnal variation is demonstrated through a direct comparison of observations made around local noon and approximately 12 hours later. Emphasis is given to the decoupling of the boundary layer during the morning into a separate cloudy layer and surface mixed layer.

1. Introduction

It is now well recognized that the extensive areas of marine stratus and stratocumulus clouds that are a persistent feature of the eastern parts of the major ocean basins are likely to exert a strong influence on climate and possible climate change. The high albedo of these clouds, relative to the sea surface, leads to a substantial deficit in the total absorption of solar radiation in any vertical column, compared to a cloud-free area. Furthermore, because of their low altitude there can be little compensation to the net radiation budget from the cloud-top longwave flux. Through these important radiative exchanges low-level clouds have a significant influence on the resulting surface energy balance and, hence, on the determination of surface fluxes of heat and moisture. In recognition of these factors the First International Satellite Cloud Climatology Project Regional Experiment (FIRE) was conceived as a multidisciplinary approach to the problem of obtaining a very large dataset intended to improve knowledge and understanding of the dominant physical processes occurring in marine stratiform clouds. The various strategies to be adopted and goals pursued are described by Randall et al. (1984). In this paper observations are presented of diurnal change in the turbulent structure of the cloudy marine boundary layer; the measurements were made during the FIRE intensive observing period in the summer of 1987 using instruments attached to the cable of a tethered balloon.

The important physical processes operating within a cloud-capped boundary layer and the current state of knowledge, in both modeling and observations, have recently been thoroughly reviewed by Driedonks and Duynkerke (1989), whose paper contains a comprehensive list of relevant references. Briefly, in summarizing the processes at work in cloud-capped boundary layers, an idea frequently encountered is that of longwave cooling at cloud-top driving turbulent mixing throughout the depth of the boundary layer, even in the absence of significant surface fluxes. This cloud-top cooling supports a positive vertical buoyancy flux through the boundary layer and maintains it in a well-mixed state. The vertical extent of the radiative cooling, however, is limited to a shallow region, perhaps a few tens of meters deep adjacent to the top of the cloud. Associated with this generation of turbulent energy, albeit in a rather complex manner, is the entrainment of warmer unsaturated air from the inversion layer above. Dependent upon the degree and manner of the subsequent mixing, entrainment is potentially a mechanism for drying and hence thinning the cloud layer.

In contrast to the longwave cooling, the heating which results from absorption of shortwave solar radiation is distributed more deeply in the cloud layer. As a result, even though the shortwave heating when averaged over a vertical column may approximately balance the longwave cooling, the vertical distribution of heating and cooling can serve to destabilize the cloud layer alone, independently of the rest of the boundary layer. The net result of the combined entrainment, shortwave heating and longwave cooling may be that the cloud layer is warmed relative to the subcloud layer. This implies the formation of a stable layer, which serves to limit the vertical extent of mixing from the surface and reduces transport between the upper and lower parts of the boundary layer. This decoupling of the cloud layer from the rest of the boundary layer substantially reduces the turbulent fluxes into the cloud. To maintain the cloud against the drying effect of en-

Corresponding author address: Dr. P. Hignett, The Met. Office Research Unit, Royal Air Force Cardington, Bedford MK42 OTH, United Kingdom.

trainment and shortwave heating a supply of moisture from the surface is required. However, after decoupling this supply is greatly reduced and a substantially enhanced thinning of the cloud may be expected. The modeling work of Turton and Nicholls (1987) and Duynkerke (1989) implies this decoupling occurs several hours before local noon. In the afternoon the layers may reconnect with a subsequent thickening of the cloud layer. From an analysis of radiosonde measurements made during the FIRE observing period, Betts (1990) concludes that a strong diurnal variation was present, connected with the daytime decoupling of the boundary layer.

Section 2a of this paper describes the island location of the surface-based measurements made during FIRE and a description of the cloud layer on the particular day to be studied here. The instruments used for turbulence measurements from a tethered balloon are described in section 2b. The presentation of the results in section 3 concentrates initially on a direct comparison between observations made around midday and midnight; this is then extended to the time variation in the boundary layer structure during the morning.

2. Location and instrumentation

a. Cloud description

As part of the 1987 FIRE intensive observing period a comprehensive array of surface-based instrumentation was deployed on San Nicolas Island (SNI), about 105 km off the coast of Southern California, at approximately 33°15′N, 119°30′W. The island is about 15 km by 4 km with its major axis lying along the most frequent wind direction, which is northwesterly; because of this observations from the island are often characteristically those of a marine boundary layer. Randall et al. (1984) estimate SNI lies within a marine boundary layer approximately 50% of the time. SNI is an established meteorological site and has been used for previous marine boundary layer studies (e.g., Blanc 1981; Davidson et al. 1984). A combination of these qualities and the high fractional low-cloud cover (51% in July) made SNI an excellent choice for a surface-based marine stratocumulus study.

The particular instruments that will be of interest here were a Doppler acoustic sounder (operated by Pennsylvania State University; White 1989), a laser ceilometer (operated by Colorado State University; Schubert et al. 1987) and a passive microwave radiometer for the measurement of column water vapor and liquid water amount (operated by NOAA/Environmental Research Laboratories; Snider 1988). These were positioned on the northwest promontory of the island at approximately 15 meters above sea level.

The data to be presented in later sections were taken during the period between 1640 UTC 14 July and 0800 UTC 15 July (all subsequent times will be assumed to be UTC). There was little change in the general synoptic pattern over this period, with west-northwesterly winds being maintained in the experimental area. A detailed description of the cloud conditions on the day and night of 14/15 July can be found by reference to Fig. 1. This diagram shows time series of cloud top height (derived from peak acoustic echo strength measurements; White 1989), cloud base from the ceilometer (courtesy of Professor Wayne Schubert) and liquid water path (courtesy of Dr. Jack Snider); the plots are based on 10-minute averaged data. The overall picture is of a cloud layer that progressively thins during the late morning and into the afternoon, both by raising the cloud base and lowering the inversion, but thickens again during the evening and overnight. Although the cloud layer did not break completely it became very thin around 0000 and could probably not at this point be considered to act as a blackbody for longwave radiation (Stephens 1978). Radiosonde ascents and aircraft observations indicated that there was no upper cloud present.

Two periods were selected for detailed comparison and are indicated on Fig. 1. The first is around local noon, and the second close to local midnight. The mean inversion height in both cases is very similar, and although both sections lie within an overall trend, in neither case does the change exceed about 10%. The liquid water path varies by a factor of about two but in both cases remains sufficient to ensure that the cloud acts as a blackbody in the far-infrared. The mean wind velocity, averaged over $0.2Z_i$ to $0.9Z_i$, (where Z_i is the inversion height) was 6.2 m s^{-1} at 293 deg for the daytime period and 6.2 m s^{-1}, 291 deg at night. The similarity of inversion heights and wind velocities, combined with the lack of significant change in sea surface temperatures, provides the opportunity to make the most direct assessment so far of the variation in the boundary layer structure over a half-solar cycle,

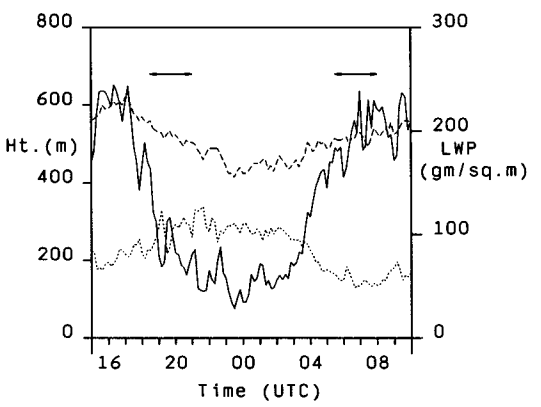

FIG. 1. Liquid water path, LWP, (full line) and height of cloud top (dashed line) and cloud base (dotted line) against time from 1500 UTC 14 July to 1000 UTC 15 July. The arrows denote the periods selected for direct comparison. Local noon occurred at 2004.

while other conditions change little. The observation that the various quantities on Fig. 1 show no significant net change over approximately a day gives some confidence to the neglect of any advective effects, which necessarily arises from making measurements at a single point.

b. *Turbulence measurements*

Turbulence measurements were made using instruments attached to the tether cable of a 1076 m^3 helium-filled kite balloon operated by the NASA Wallops Flight Facility. The mooring point for the balloon was 30 m above sea level, approximately 400 m downwind of the shore line and 300 m from the other surface-based instruments. Blanc (1981), using the results of Frost et al. (1974), estimated the influence of this slope on the local wind field. At the lowest heights at which measurements were made (approximately 100 m AGL) the anticipated speedup in the wind is about 1% to 2%, a factor too small to be detectable. At the surface the largest typical speedup is about 5%.

The turbulence probes, their response and method of operation are described by Lapworth and Mason (1988). Briefly, each probe consists of a main rectangular housing containing inclinometers for the measurement of pitch and roll angles, an aneroid pressure transducer, signal conditioning and encoding electronics, a low power 400 MHz radio transmitter and rechargeable batteries that give an operating time of typically 8 to 10 hours. This housing is clamped to the tether cable, a steel wire rope, and is free to rotate around it under the action of a tail-mounted vane. The relative wind vector is determined from three Gill propeller anemometers attached to the front of the housing and arranged in a cone with opening angle of 60°.

The orientation of the probe, relative to the earth's magnetic field, is measured by a three-axis flux-gate magnetometer; data from this and the inclinometers are used to rotate the relative wind velocity into a ground-based frame of reference. The propeller array also surrounds a platinum resistance thermometer for fast-response temperature measurements. A psychrometer employing wet and dry thermistors is used for the measurement of humidity. The sensor outputs are sampled at ~21 Hz and the digitized encoded data transmitted to the surface.

A disadvantage of a tethered balloon as an instrument platform is that it is in constant motion in the same range of frequencies as those it is wished to measure. These motions arise from that of the balloon itself, acting as an upside-down pendulum, and vibrational modes of the tether cable. Corrections can be derived by combining information from the inclinometers and magnetometers to deduce the vector orientation of the cable at each probe position; this allows the approximate shape of the cable to be determined and from this follows the position of each probe relative to the tether point. The variation with time of this position allows the measured wind velocities to be corrected for probe motions.

On 14/15 July measurements were made during the day and, after a break for battery charging and topping up the balloon, again for a time overnight. Six probes were available for the daytime measurements and five for the night. Data were recorded for periods of typically just over an hour with the balloon at constant height. The intention was to keep a minimum of one probe at or just above cloud top; between runs small changes in balloon height were necessary to accommodate changes in inversion height. The other probes were arranged at various heights between cloud top and about 100 meters AGL. An advantage of the tethered balloon over an instrumented aircraft is the ability to make measurements over an extended period throughout the day or night. Furthermore, since multiple level measurements can be made simultaneously, a degree of vertical coherence can be maintained.

3. Results

a. *Data reduction*

Limitations on the volume of data storage available meant that data were recorded by sampling every fifth reading to give an effective recording rate of 4.15 Hz. However, this does not imply potential problems from aliasing as the response of the transducers has also to be considered. For example, the Gill propeller anemometers have a length constant for axial flow of ~1 meter. At the typical wind speeds encountered, ~6 m s^{-1}, this gives an effective frequency response of ~6 Hz. There is a further electrical low-pass filter at 10 Hz [see Lapworth and Mason (1988) for a further description of the probe signal conditioning] and hence minimal scope for aliasing of frequencies higher than the recording rate, which is nevertheless sufficient to resolve the turbulent motions at the heights considered. The data were then arranged into 33 minute segments for further processing. After calibration the wind velocity components, corrected for probe motions as described above, were derived and rotated into a right-handed coordinate frame with the horizontal axes aligned along and perpendicular to the mean wind direction. Linear trends were removed from these time series before the calculation of variances, covariances and the accompanying power spectra and cospectra.

b. *Mean profiles*

The day and night periods selected for a direct comparison correspond to 1830–2100 for the daytime and 0530–0800 for the night. Local noon occurred at 2004; hence, the daytime data were taken when the solar zenith angle was changing only slowly. From the individual data segments the mean values of virtual potential temperature (θ_v), wind speed and direction were

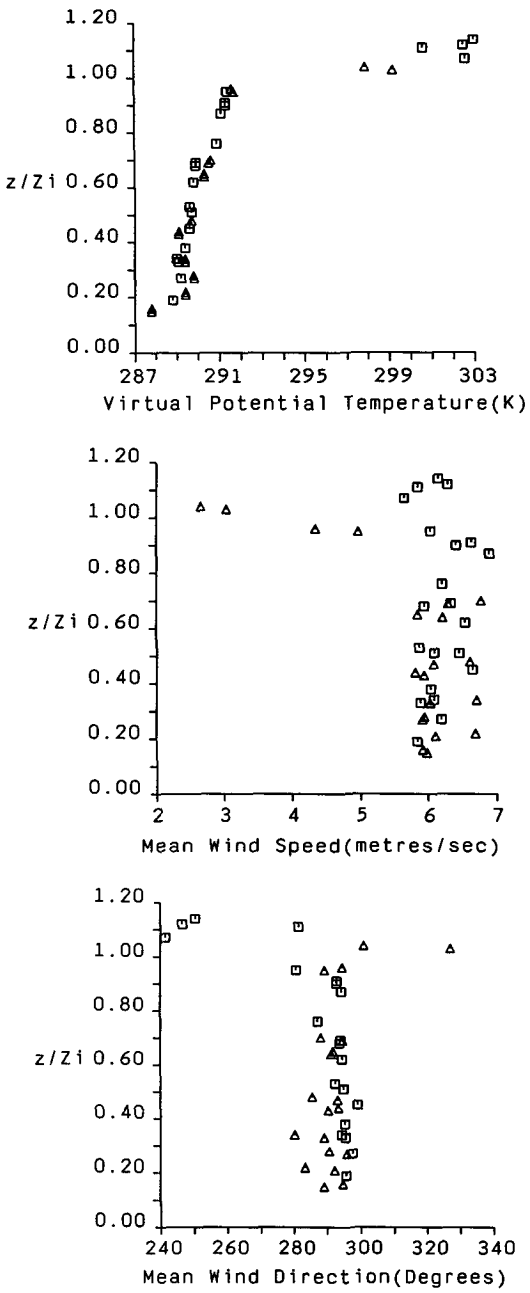

FIG. 2. (a) Virtual potential temperature against height (normalized by the inversion depth, Z_i) for the daytime period (squares) and nighttime (triangles). (b) As in (a) except for mean wind speed. (c) As in (a) except for mean wind direction.

calculated and are plotted without respect to time in Figs. 2a–c, respectively. The ordinate is height above sea level, normalized by the mean inversion height, which is inferred from the temperature structure recorded by the probes maintained around cloud top. A well-marked inversion, of ~10 K, can be seen in Fig. 2a; below this little systematic variation between day and night is apparent. Although the equivalent potential temperature (θ_e) would be a better choice as a conservative variable than θ_v, the absolute accuracy of its calculation is much lower because of the sensitivity of θ_e to humidity variations. Although fluctuations in θ_e are used satisfactorily in the flux data presented later an unacceptable degree of scatter arises from combining mean θ_e values from different probes; this comes from inevitable small difference in absolute calibration and results in the choice of θ_v for the mean profiles. The wind speed and direction in Figs. 2b and 2c further give the impression of a boundary layer that is basically well-mixed but without revealing any detailed structure. There is evidence of considerable low-frequency variability, between day and night, of the wind velocity in the inversion layer leading to the development of substantial shears. The role of this wind shear in promoting entrainment through the local generation of turbulence is as yet unclear (Driedonks and Duynkerke 1989).

c. *Turbulence structure*

To use as an indicator of convective activity the vertical velocity variances were calculated for the day and night periods and are plotted against normalized height on Fig. 3; also this diagram shows the range of cloud-base height measured by the ceilometer. The daytime profile shows characteristically low values above cloud, a distinct maximum in the cloud layer, and evidence of a second weak maximum below. This profile shape is similar to that shown by Nicholls (1984) and is consistent with mixing being driven from the surface and cloud top. In contrast, although having more individual scatter, the nocturnal data have the appearance of a more intensely turbulent layer well mixed from inversion to surface and driven from cloud top in a manner analogous to that of a convective boundary layer heated from below (e.g., Lenschow et al. 1980). These features are also reflected in the behavior of the equivalent po-

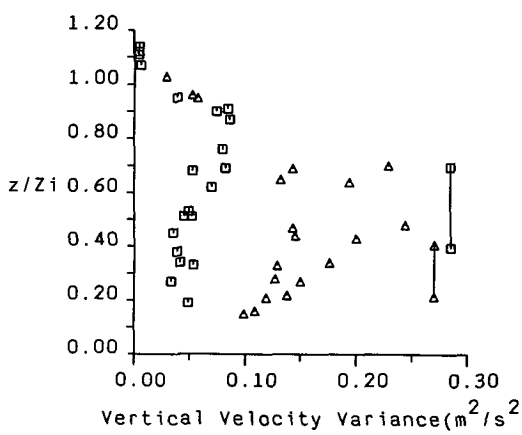

FIG. 3. Vertical velocity variance against height (normalized by the inversion depth, Z_i) for the daytime period (squares) and nighttime (triangles). The pairs of symbols connected by lines denote the range of cloud base height during each period.

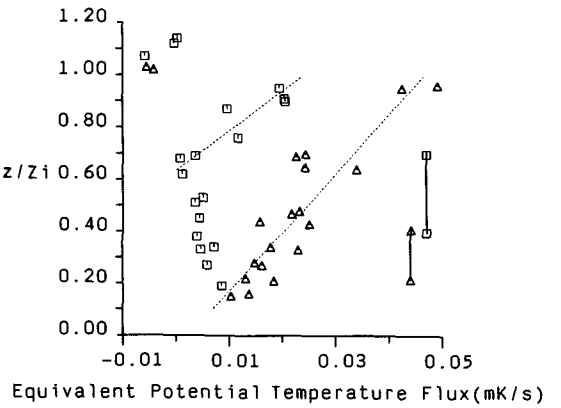

FIG. 4. As in Fig. 3 except equivalent potential temperature flux. The dotted lines are simple best fits to the daytime cloudy mixed layer and the nocturnal mixed layer.

tential temperature flux shown in Fig. 4. In both cases the profiles tend to a weak positive surface flux, and the flux maxima are located close to cloud top, with the larger fluxes occurring at night. However, whereas the nocturnal data again give the appearance of a single mixed layer driven by a cloud-top buoyancy flux, the daytime profile has a distinct minimum value around zero in the lower part of the cloud layer.

The daytime boundary layer around local noon appears to consist of a cloudy mixed layer surmounting a mainly subcloud layer driven from the surface. This is reminiscent of the results of the JASIN experiment (e.g., Slingo et al. 1982; Nicholls 1985) where the surface mixed layer had a depth $\approx 0.2u_*/f$. Here u_* is the friction velocity and f the Coriolis parameter; u_*/f is therefore an Ekman scale such that in a neutral atmosphere a steady, neutral boundary layer could be expected to establish a depth of $\approx 0.35u_*/f$. These results imply strongly that the daytime boundary layer is decoupled in the sense described by Nicholls (1984) and are consistent with the conclusions of Nicholls and Leighton (1986). The top of the surface layer and the base of the cloudy mixed layer are not clearly associated with cloud base, which tended to be variable and ill-defined. However, the upper limit of cloud base, as shown on Figs. 3 and 4, does tend to coincide with the top of the surface mixed layer.

If the daytime cloud layer and the complete nocturnal boundary layer are examples of convectively driven mixed layers then both should exhibit the same similarity. Although there is unlikely to be a universal scaling applicable to cloudy convective layers, a simple approach can be adopted by redefining the height coordinate as distance from cloud top and normalizing by the appropriate mixed layer depth. Following Nicholls and Leighton (1986) the vertical velocity variances were scaled with a convective velocity scale defined as $w_* = (gh\, w'\theta_v'/\bar{\theta}_v)^{1/3}$. For the nocturnal data the mixed layer depth, h, is taken as the full depth of the boundary layer; for the daytime data h is the depth of the cloudy mixed layer, estimated from the flux and variance profiles. Hence, data from the daytime surface mixed layer is excluded. The values of virtual potential temperature flux ($w'\theta_v'$) used in the definition of w_* were simply taken as those appropriate to cloud top and were estimated as 9.8×10^{-3} m s^{-1} K and 1.7×10^{-2} m s^{-1} K for the daytime and nocturnal data, respectively. The resulting scaled mixed-layer variances are plotted in Fig. 5 with a curve derived by Lenschow et al. (1980) (and plotted upside down) from measurements in convective boundary layers over land. The overall scatter is similar to that shown by the data of Nicholls and Leighton (1986) and confirms that, on the whole, the curve is a reasonable description of the overall variability away from the boundaries. Without substantially more data it would be unwise to infer much from any apparent differences between the day and night data. However, the lowest daytime values do appear to deviate significantly and are presumably indicative of the difference in the lower boundary condition of the two mixed layers. The equivalent potential temperature fluxes were scaled simply with the cloud-top maxima, derived by a simple best-line fit to the profiles of Fig. 4. The resulting normalized flux data are plotted in Fig. 6, where they show a reasonable collapse and, within the scatter, can be adequately described by a simple linear dependence on distance from cloud top.

A result which may be anticipated from the day to night variation of the mixed layer depth (a factor of about 3) is that the turbulent length scales should also show a substantial variation. A representative length scale can be estimated from the wavelength of the peak in the vertical velocity spectra. The spectra are illustrated in Fig. 7, which shows the spectral estimates, normalized by the variance, weighted by the wavenumber and averaged into ten bins per decade, and are plotted against the wavenumber normalized by the

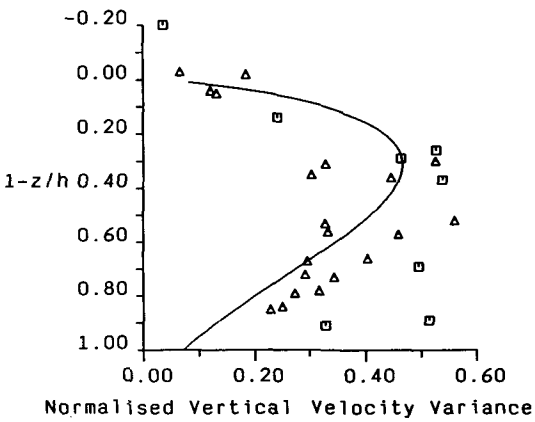

FIG. 5. Vertical velocity variance (normalized by the convective velocity scale) against distance from cloud top (normalized by the mixed layer depth, h); daytime period (squares) and nighttime (triangles). The full curve is from Lenschow et al. (1980), plotted upside down.

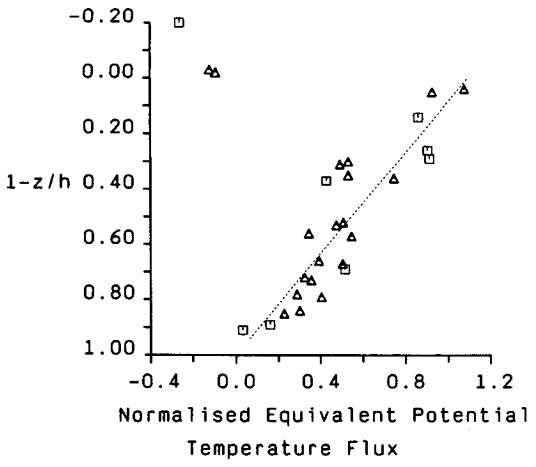

FIG. 6. Equivalent potential temperature flux (normalized by the cloud top flux) against distance from cloud top (normalized by the mixed layer depth, h). The dotted line is a linear best fit to the data below cloud top.

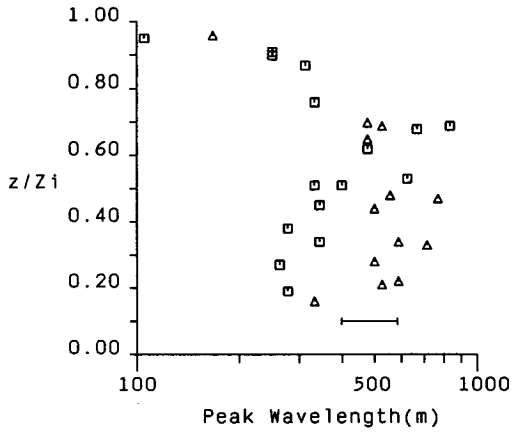

FIG. 8. Peak wavelengths of the vertical velocity spectra against height (normalized by the inversion depth, Z_i); daytime period (squares) and nighttime (triangles). The error bar is an estimate of the uncertainty involved in deriving the wavelengths.

mixed layer depth. The wavenumber has been derived via the mean wind speed using Taylor's hypothesis. In terms of $(1 - z/h)$ the spectra cover the range 0.2 to 0.8. A single peak is apparent and at high frequencies the data tend to a single curve of slope $-\frac{2}{3}$. Although considerable low-frequency variability is evident, the remainder of the spectra show little change in shape and make the dominant contribution to the variance. Note that there will not be the complete collapse of the spectra, particularly in the inertial subrange, that would be anticipated if the full mixed-layer scaling of Kaimal et al. (1976) were used.

The turbulent length scales were estimated subjectively by eye, and the results plotted against normalized height on Fig. 8. A logarithmic scale is used for the length scale to reflect the fact that the data were extracted from logarithmic spectral plots. In the lower half of the boundary layer the day and night data separate into two distinct groups; in the upper half the reduction in length scale as cloud top is approached can be seen. The nocturnal length scales and those from the daytime cloudy mixed layer were scaled with the corresponding mixed layer depth and plotted against $(1 - z/h)$. In Fig. 9 they are compared with a curve derived by Kaimal et al. (1976) from observations of convective mixed layers over land. The agreement is reasonable (cf. Nicholls 1989) with significant deviations becoming apparent at the lower reaches of the mixed layers. If the depth of the surface mixed layer is d, Nicholls (1985) suggests that if $0 < -d/L < 2$ (where L is the Monin-Obukhov length) mixing from the surface will be limited to a height $\sim 0.2u_*/f$ if there is no intervening inversion. No direct measurements of surface fluxes were made and a best estimate of $-d/L$ is ~ 1, with a probable uncertainty of ± 1. This lies within the appropriate range and suggests that a com-

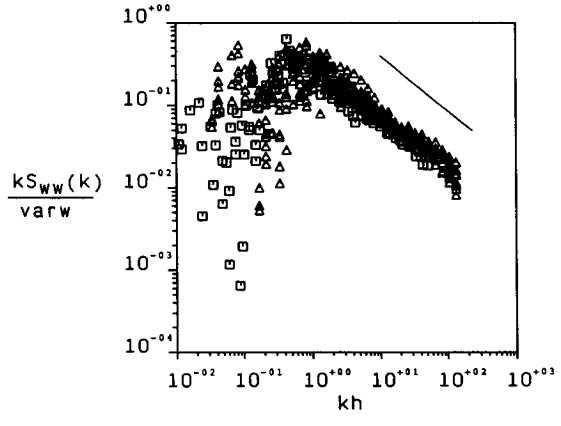

FIG. 7. Power spectra of the vertical velocity component normalized by the variance (varw); k is the horizontal wavenumber, h the mixed layer depth; daytime period (squares), nighttime (triangles). The straight line has a slope of $-\frac{2}{3}$.

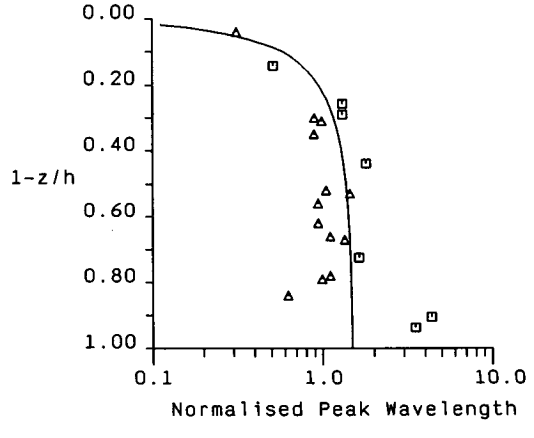

FIG. 9. Peak wavelengths of the vertical velocity spectra against distance from cloud top (both normalized by the mixed layer depth, h); daytime period (squares), nighttime (triangles). The curve is a result from Kaimal et al. (1976) and is here plotted upside down.

parison may be made with Nicholls' (1985) observation that the turbulent length scale in the surface mixed layer, corrected for stability, should scale with height above the surface. The length scales were corrected using Nicholls' expression for the stability dependence, expressed as a function of u_*/fL, although there will be a remaining systematic variation arising from the uncertainty in L. Although the height range available is rather restricted, the results shown in Fig. 10, where the length scales and heights have been normalized by u_*/f, compare favorably with the suggested simple linear relationship. Furthermore, the depth of this layer is $\sim 0.2u_*/f$, which is indicative that this height scale is relevant in subtropical regions, as employed by Brost et al. (1982a), as well as the midlatitude areas where most studies have been conducted. More observations under a wider range of conditions will be needed to confirm this.

Some estimates of the accuracy of the statistics can be made by reference to Lenschow and Stankov (1986). If their averaging lengths are interpreted as averaging periods, this implies that a 10% accuracy for the vertical velocity variance requires typically 25 minutes for mixed layer depths corresponding to a decoupled boundary layer and ~70 minutes for the full boundary layer depth. Hence, the averaging period used to present the data, ~33 minutes, should meet this requirement for the shallow decoupled layers but any shortfall may explain some of the greater scatter seen in the nocturnal data.

d. Decoupling

The results presented so far demonstrate that despite the considerable variation in cloud structure over half a day, the changes are sufficiently slow around midday and midnight that the turbulent structures of the boundary layer can be compared directly with each other and with the results of earlier aircraft and modeling studies. In particular, the decoupled structure of the daytime boundary layer is very apparent. By examining the data taken earlier in the morning, it may be possible to detect the change in turbulent structure of the boundary layer as the decoupling occurs; this would be extremely difficult to accomplish with an instrumented aircraft. A mixed-layer timescale can be estimated as $t_* = h/w_*$, where taking typical nocturnal values of $h \approx 500$ m and $w_* \approx 0.5$ m s^{-1} gives $t_* \approx 1000$ s which reduces to t_* 500 s for a daytime decoupled cloudy layer. This implies that once sufficient stabilization has occurred for the single mixed layer structure to be disrupted, the reorganization of the new cloud and surface mixed layers should occur on timescales shorter than the typical averaging period used (~2000 s). With this in mind, data from the first two data segments beginning at 1640 were examined. The vertical velocity variances are plotted against normalized height on Fig. 11. Comparison of these profiles with Fig. 3 reveals a structure that for the first of these segments is similar to the nocturnal profiles; however, by the second segment the profile has adopted the character of the data recorded later in the day. It would appear that the boundary layer may have decoupled during the period from ~1640 to 1750, but sufficiently rapidly that although the absolute magnitude of the variance estimates in Fig. 11 may be in some doubt their relative values should be reliable.

This change in structure characteristic of the cloud-layer decoupling can be emphasized by examining the length scales as before. The peak wavelengths from the vertical velocity spectra for these first two segments are displayed in Fig. 12. The behavior here is very similar to that shown on Fig. 8; from the first to the second segment there is a general reduction in the length scales, with a large reduction in the lower half of the boundary layer. This is consistent with a decoupling into cloudy and surface mixed layers, with the turbulence taking up the length scales consistent with the new mixed layer depths. For small z/Z_i the length scale from the first

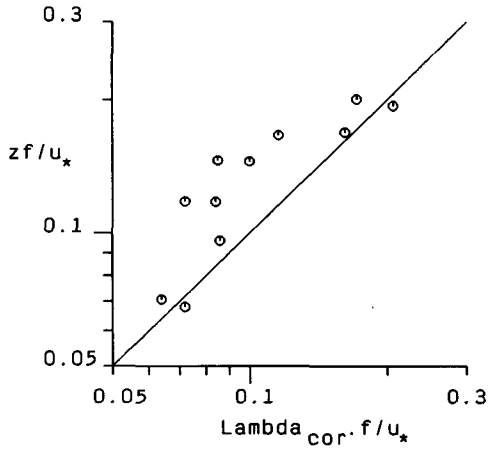

FIG. 10. Corrected peak wavelengths (Lambda$_{cor}$) surface mixed layer plotted against height, both normalized by u_*/f. See section 3c for details of derivation of wavelengths; the straight line represents a linear scaling of wavelength with height.

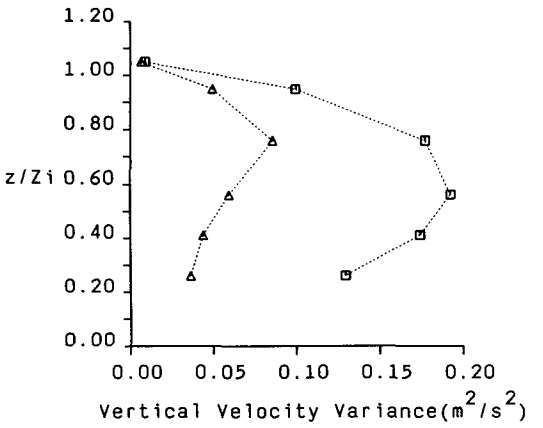

FIG. 11. Vertical velocity variance against normalized height for data segments beginning 1640 (squares) and 1713 (triangles).

segment, when a single mixed layer is anticipated, should tend to $\sim 1.5Z_i$, or ~900 meters as observed (Kaimal et al. 1976). However, if the surface mixed-layer scaling applies, then the length scale at the lowest measurement level (at which $z \sim 0.1\, u_*/f$) should, by reference to Fig. 10, be ~200 meters—again as observed.

Subsequent to the change apparent in Figs. 11 and 12 there is the large drop in liquid water path seen in Fig. 1 after ~1700; this is consistent with a marked reduction in the humidity flux into the cloud layer after decoupling occurs. It might also be expected that a warming of the cloudy layer relative to the surface mixed layer would occur, even though this may be only ~0.5 K (Turton and Nicholls 1987). By examining the changes in temperature at each probe position, the relative warming should be detectable. This procedure should eliminate systematic differences between probes, which could otherwise mask small changes. The change in θ_v at each of the five probes below cloud top from the first to the second averaging period is plotted in Fig. 13. There appears to be a maximum warming in cloud of ~0.3 K implying a relative stabilization of this layer. Small net changes in the height of the probes, caused by variation in the wind at the height of the balloon, can account for changes in θ_v of ~0.02 K at most.

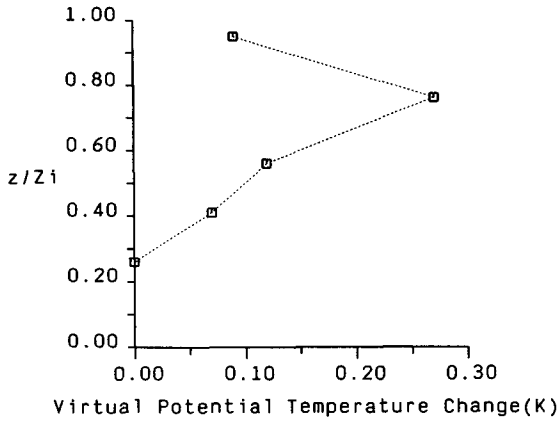

FIG. 13. Change in virtual potential temperature at each probe level from the data segment beginning 1640 to that beginning 1713, against normalized height.

4. Discussion

Detailed measurements have been presented of the structure of a cloudy marine boundary layer during the 1987 FIRE intensive observing period. Multiple-level turbulence measurements made simultaneously from a series of probes attached to the cable of a tethered balloon have demonstrated the daytime decoupling of the boundary layer into separate cloudy and surface mixed layers. The comparison between periods around noon and midnight is the most direct of this type accomplished so far and demonstrates the potentially dominating influence of solar radiation on the structure of a cloud-capped boundary layer. The nature of the decoupling and the mixed layers subsequently formed is very similar to the observations previously reported by Nicholls (1984) and Nicholls and Leighton (1986). However, the diurnal variation implicit in these aircraft observations arises from a composite view constructed from several cases studied over a few years. The marked variation reported in this study was observed within a day and demonstrates the large changes in the magnitude of the turbulent quantities that can occur without a significant change in the surface conditions. A conveniently defined turbulent length scale has been shown to be an effective diagnostic quantity in deducing the structure of the boundary layer. It has also been possible to demonstrate the changes that occur at the decoupling process during the morning, an observation not previously possible.

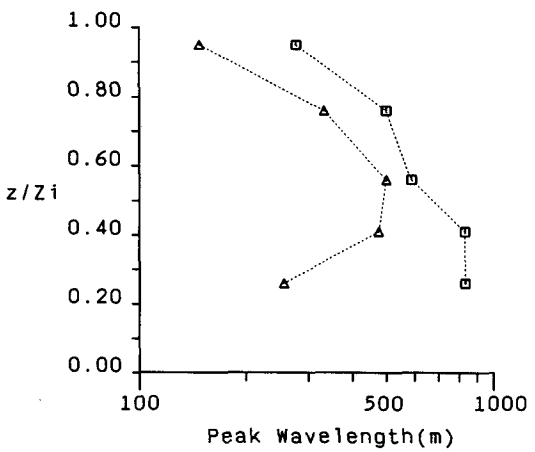

FIG. 12. As in Fig. 11 except for peak wavelengths of the vertical velocity spectra.

Many previous observations have been made in midlatitudes and some differences with the current subtropical clouds remain. Midlatitude clouds often have tops at around 1000 m or higher, consequently the surface mixed-layer depth can be much less than the inversion height and may not reach to cloud base. The daytime decoupled boundary layer may therefore be deep enough to have an identifiable stable layer between the cloudy and surface mixed layers. Furthermore, the decoupling can be readily associated with the cloud base and immediate subcloud layer. In the observations presented in this paper cloud tops were typically around 500 m with the surface mixed layer ~350 m or higher. After decoupling the division between the cloudy and surface mixed layers was not clearly associated with cloud base, and it is doubtful whether under these circumstances a completely unambiguous identification of the formation of a stable layer could be made.

The observations of Brost et al. (1982a,b), although made in a geographically similar region to the present study, were of cloudy boundary layers dominated by

shear production of turbulent kinetic energy rather than buoyant production. Expressed in a different way, the surface mixed-layer depth scale ($d = 0.2u_*/f$) was approximately twice the inversion height. Therefore, turbulent mixing from the surface could be supported up to cloud-top, thus precluding the possibility of any decoupling into separate layers. Similarly for the single strong wind case of Nicholls and Leighton (1986), which was also dominated by shear production, $d/Z_i \approx 1.4$; for those cases which these authors diagnosed as decoupled then $d/Z_i < 1$, as was the case in the present study. Similarly the period discussed by Betts (1990) was characterized by $d/Z_i < 1$. However, this cannot be taken as a sufficient condition for decoupling to occur as a significant surface buoyancy flux can still help maintain the boundary layer in a fully mixed state.

It has not been the purpose of this study to examine the small-scale processes occurring at cloud-top, including entrainment. Similarly, little attention has been paid to the mean structure of the boundary layer, or possible departures from horizontal homogeneity; rather, the intention has been to use characteristics of the turbulent statistics effectively as indicators of the response of the boundary layer to changes in the forcing linked to the solar cycle. The description has been in terms of established mixed layer scaling, which works well without a detailed knowledge of the processes at cloud-top, a complex region that is still poorly understood. There are strong qualitative similarities with the results of modeling studies; those of Turton and Nicholls (1987) and Duynkerke (1989) predict decoupling to occur a few hours earlier than was observed and show changes in cloud-top height of about 50 meters over a diurnal cycle. This variation is smaller than that observed on the day examined here and is linked to the change in entrainment rate that accompanies the changes in the turbulent kinetic energy balance during the diurnal cycle. How much of these differences can be accounted for by appealing to the non-ideal conditions under which observations are inevitably made and how much results from inadequacies in the various model formulations is as yet unclear. It is hoped, however, that these observations and others gathered throughout the FIRE project will provide at least some of the necessary information to address these problems.

Acknowledgments. Numerous people have been involved in the planning and execution of the FIRE project. The author would like to pay particular thanks to the following: to Dave Randall, Steve Cox, Wayne Schubert, Bruce Albrecht and the late Steve Nicholls for their support and encouragement: to Dave McDougal, Tom Owens and Doris Stroup of the FIRE project office for their never flagging enthusiasm: to Rich Dixon and colleagues for their help on San Nicolas Island: to Dave Hatton and Adrian Cook of the Meteorology Office: to the staff of the Meteorological Research Flight.

REFERENCES

Betts, A. K., 1990: Diurnal variation of California coastal stratocumulus from two days of boundary layer soundings. *Tellus*, **42A**, 302–304.

Blanc, T. V., 1981: Report and analysis of the May 1979 marine surface layer micrometeorological experiment at San Nicolas Island, California. NRL Report 8363, Naval Research Laboratory, Washington, DC., 149 pp.

Brost, R. A., D. H. Lenschow and J. C. Wyngaard, 1982a: Marine stratocumulus layers: Part I: mean conditions. *J. Atmos. Sci.*, **39**, 800–817.

——, J. C. Wyngaard, and D. H. Lenschow, 1982b: Marine stratocumulus layers. Part II: Turbulence Budgets. *J. Atmos. Sci.*, **39**, 818–836.

Davidson, K. L., C. W. Fairall, P. Jones Boyle, and G. E. Schacher, 1984: Verification of an atmospheric mixed layer model for a coastal region, *J. Climate. Appl. Meteor.*, **23**, 617–636.

Driedonks, A. G. M., and P. G. Duynkerke, 1989: Current problems in the stratocumulus-topped atmospheric boundary layer. *Bound.-Layer Meteor.*, **46**, 275–304.

Duynkerke, P. G., 1989: The diurnal variation of a marine stratocumulus layer: a model sensitivity study. *Mon. Wea. Rev.*, **117**, 1710–1725.

Frost, W., J. R. Maus and G. H. Fichtl, 1974: A boundary-layer analysis of atmospheric motion over a semi-elliptical surface obstruction. *Bound.-Layer Meteor.*, **7**, 165–184.

Kaimal, J. C., J. C. Wyngaard, D. A. Haugen, O. R. Cote, V. Izurri, S. J. Caughey and C. J. Readings, 1976: Turbulence structure in the convective boundary layer. *J. Atmos. Sci.*, **33**, 2152–2169.

Lapworth, A. J., and P. J. Mason, 1988: The new Cardington balloon-borne turbulence probe system. *J. Atmos. Oceanic Technol.*, **5**, 699–714.

Lenschow, D. H., and B. B. Stankov, 1986: Length scales in the convective boundary layer. *J. Atmos. Sci.*, **43**, 1198–1209.

——, J. C. Wyngaard, and W. T. Pennell, 1980: Mean field and second moment budgets in a baroclinic convective boundary layer. *J. Atmos. Sci.*, **37**, 1313–1326.

Nicholls, S., 1984: The dynamics of stratocumulus: aircraft observations and comparisons with a mixed-layer model. *Quart. J. Roy. Meteor. Soc.*, **110**, 783–820.

——, 1985: Aircraft observations of the Ekman layer during the Joint Air-Sea Interaction Experiment: *Quart. J. Roy. Meteor. Soc.*, **111**, 391–426.

——, 1989: The structure of radiatively driven convection in stratocumulus. *Quart. J. Roy. Meteor. Soc.*, **115**, 487–512.

——, and J. Leighton, 1986: An observational study of the structure of stratiform cloud sheets: Part I. Structure. *Quart. J. Roy. Meteor. Soc.*, **112**, 431–460.

Randall, D. A., J. A. Coakley, C. W. Fairall, R. A. Kropfl and D. H. Lenschow, 1984: Outlook for research on subtropical marine stratiform clouds. *Bull. Amer. Meteor. Soc.*, **65**, 1290–1301.

Schubert, W. H., S. K. Cox, P. E. Gesielski and C. M. Johnson-Pasqua, 1987: Operation of a ceilometer during the FIRE marine stratocumulus experiment, Colorado State University Atmospheric Science Paper No. 420, 34 pp.

Slingo, A., S. Nicholls and J. Schmetz, 1982: Aircraft observations of marine stratocumulus during JASIN. *Quart. J. Roy. Meteor. Soc.*, **108**, 833–856.

Snider, J. B., 1988: Radiometric observations of cloud liquid water during FIRE. *Proc. IGARSS '88 Symp.*, Edinburgh, Sept 1988, 261–262.

Stephens, G. L., 1978: Radiation profiles in extended water clouds. I: Theory. *J. Atmos. Sci.*, **35**, 2111–2122.

Turton, J. D., and S. Nicholls, 1987: A study of the diurnal variation of stratocumulus using a mixed layer model. *Quart. J. Roy. Meteor. Soc.*, **113**, 969–1009.

White, A. B., 1989: Temperature and humidity turbulence structure parameters deduced from sodar and radar reflectivities: an analysis of data from the marine stratocumulus phase of FIRE. M.S. thesis, Dept. of Meteorology, Pennsylvania State University, University Park, PA 16802, 137 pp.